

Electronic Supplementary Information (ESI)

An important prerequisite for efficient Förster resonance energy transfer from human serum albumin to alkyl gallate

Qing Wang, Ying Xiao, Yanmei Huang and Hui Li^a

a) College of Chemical Engineering, Sichuan University, Chengdu 610065, People's Republic of China

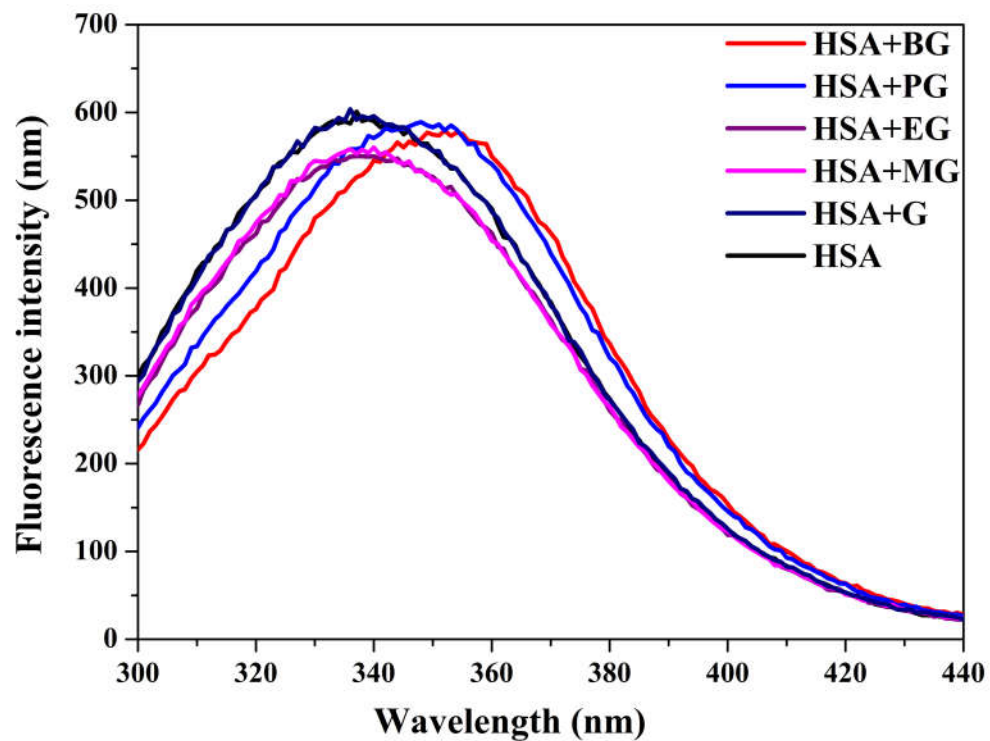


Fig. 1 Fluorescence spectra of G/ME/EG/PG/BG–HSA interaction ($\lambda_{\text{ex}} = 280$ nm). $C_{(\text{HSA})} = C_{(\text{G/ME/EG/PG/BG})} = 2 \mu\text{M}$.

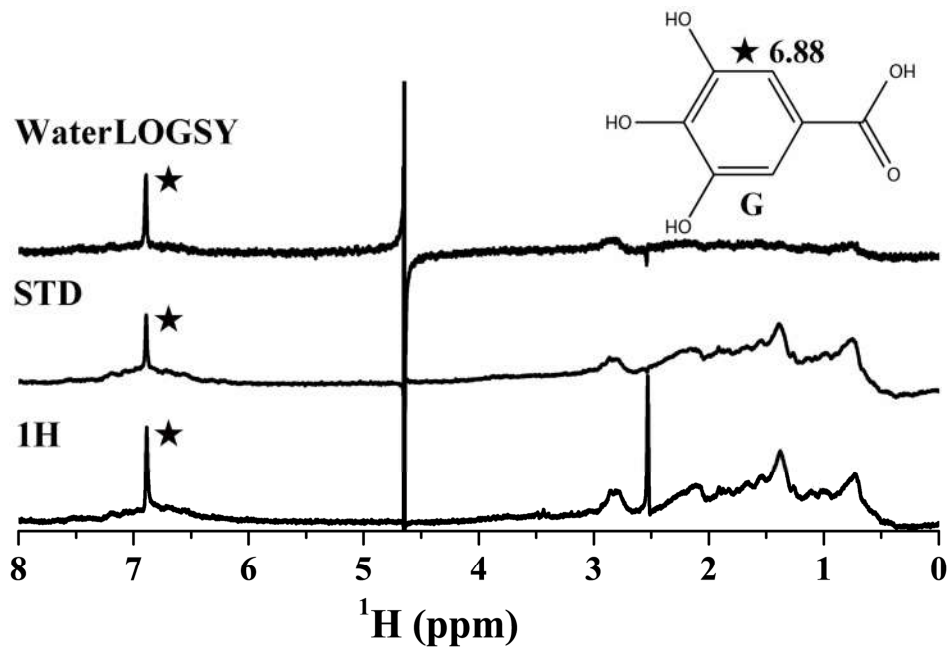


Fig. S2 The ¹H WATERGATE, STD, and WaterLOGSY spectrum for the mixture of G and HSA. $C_{(\text{HSA})} = 0.01 \text{ mM}$ and $C_{(G)} = 0.4 \text{ mM}$.

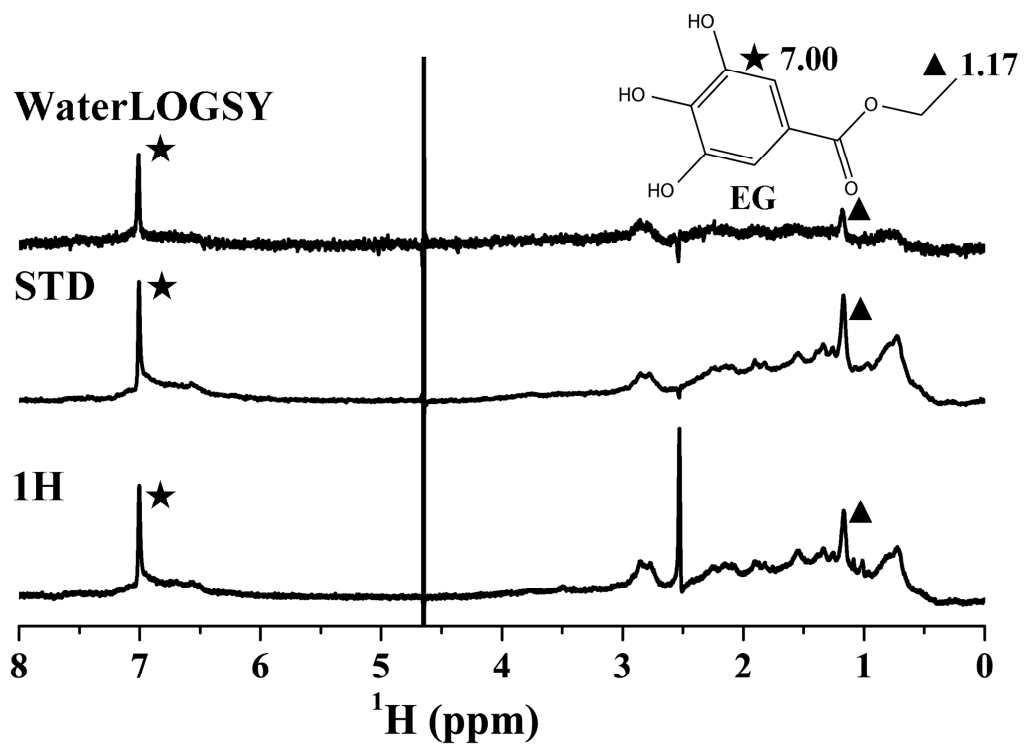


Fig. S3 The ^1H WATERGATE, STD, and WaterLOGSY spectrum for the mixture of EG and HSA. $C_{(\text{HSA})} = 0.01 \text{ mM}$ and $C_{(\text{EG})} = 0.4 \text{ mM}$.

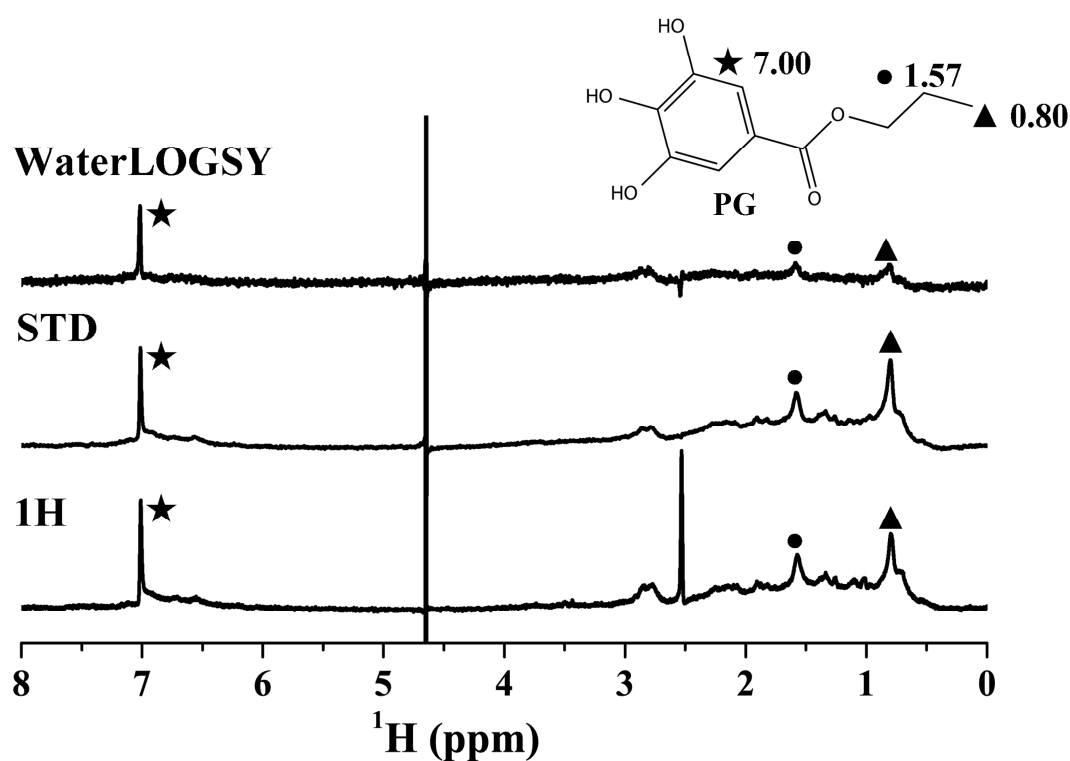


Fig. S4 The ¹H WATERGATE, STD, and WaterLOGSY spectrum for the mixture of PG and HSA. $C_{(\text{HSA})} = 0.01 \text{ mM}$ and $C_{(\text{PG})} = 0.4 \text{ mM}$.

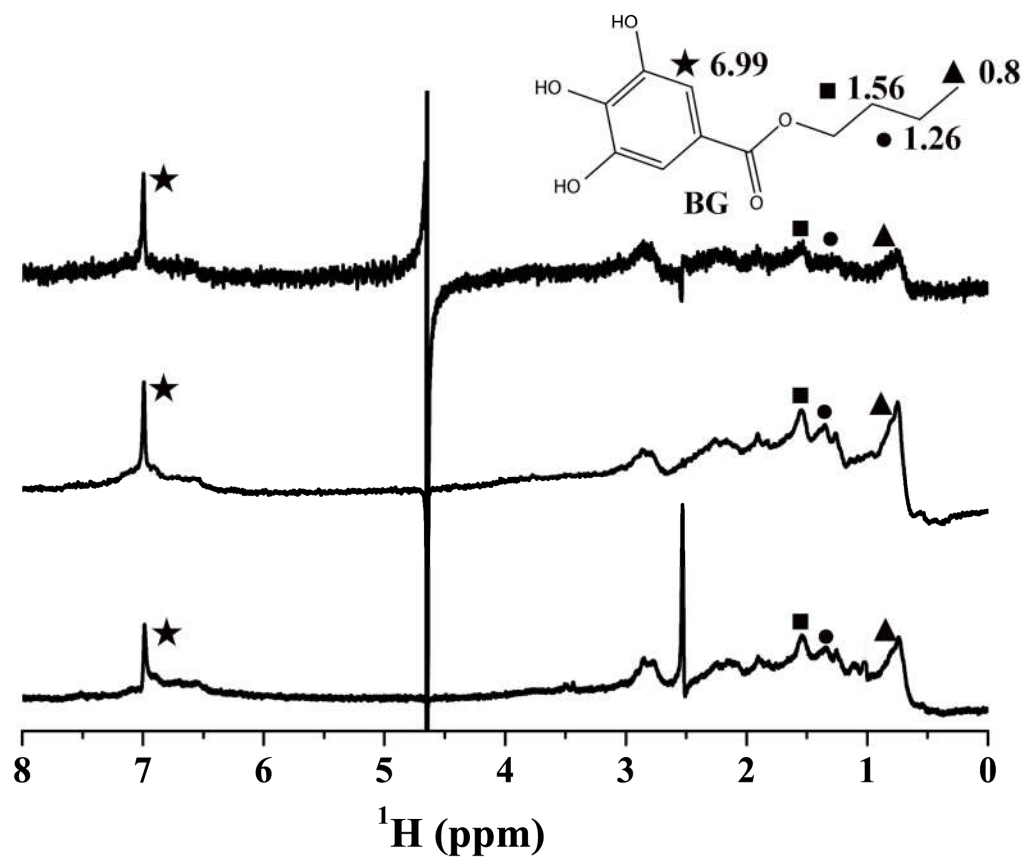


Fig. S5 The ¹H WATERGATE, STD, and WaterLOGSY spectrum for the mixture of BG and HSA. $C_{(\text{HSA})} = 0.01 \text{ mM}$ and $C_{(\text{BG})} = 0.4 \text{ mM}$.

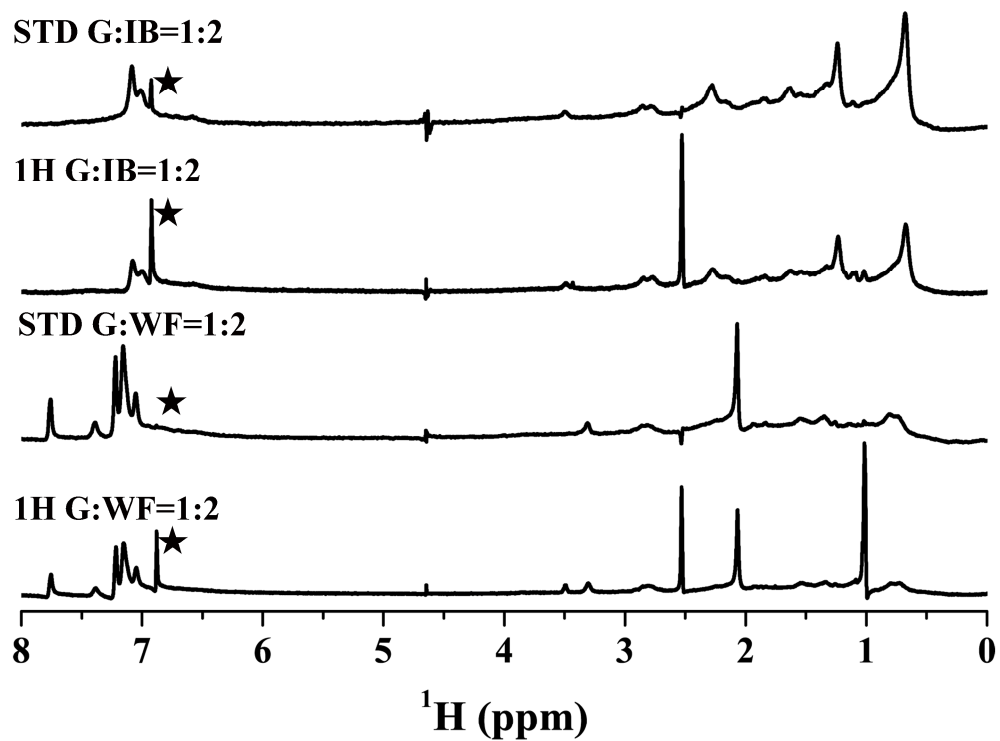


Fig. S6 Effect of WF/IB on the STD spectrum of the G-HSA interaction. $C_{(HSA)} = 0.01$ mM, $C_{(G)} = 0.4$ mM and $C_{(WF/IB)} = 0.8$ mM.

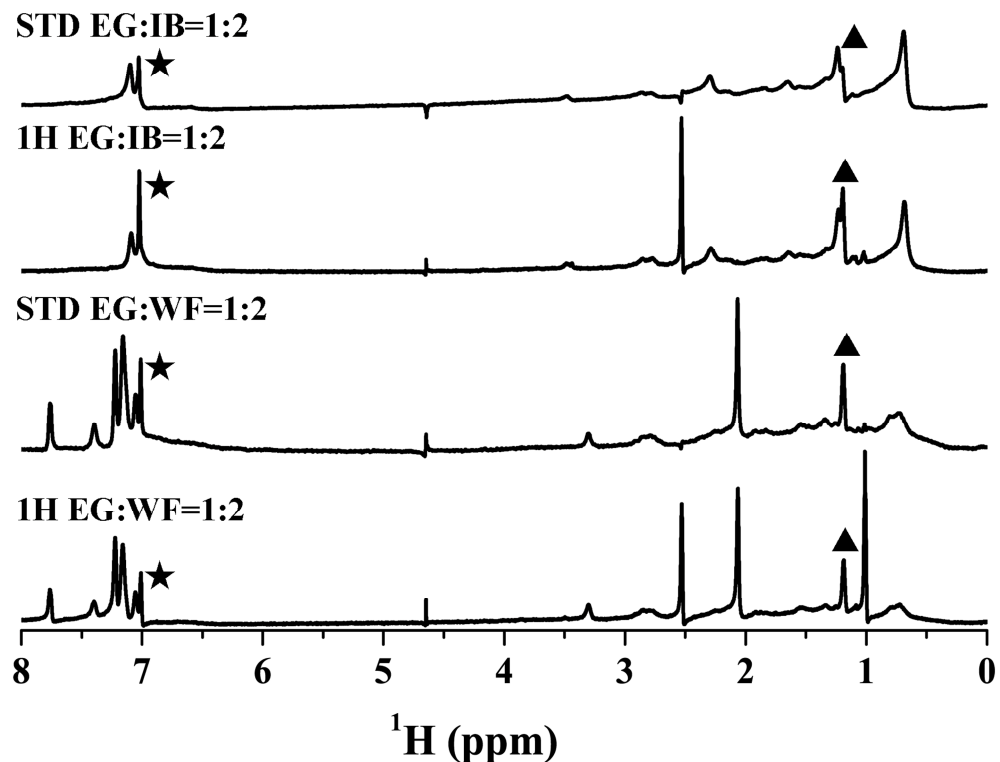


Fig. S7 Effect of WF/IB on the STD spectrum of the EG-HSA interaction. $C_{(\text{HSA})} = 0.01 \text{ mM}$, $C_{(\text{EG})} = 0.4 \text{ mM}$, and $C_{(\text{WF/IB})} = 0.8 \text{ mM}$.

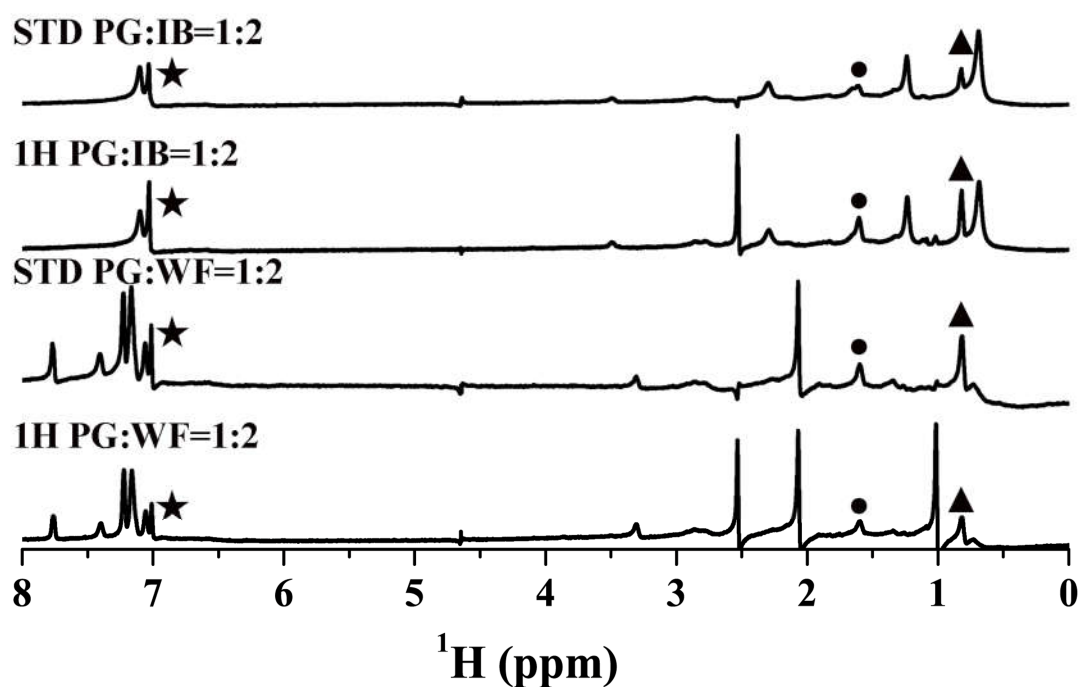


Fig. S8 Effect of WF/IB on the STD spectrum of the PG-HSA interaction. $C_{(HSA)} = 0.01 \text{ mM}$, $C_{(PG)} = 0.4 \text{ mM}$, and $C_{(WF/IB)} = 0.8 \text{ mM}$.

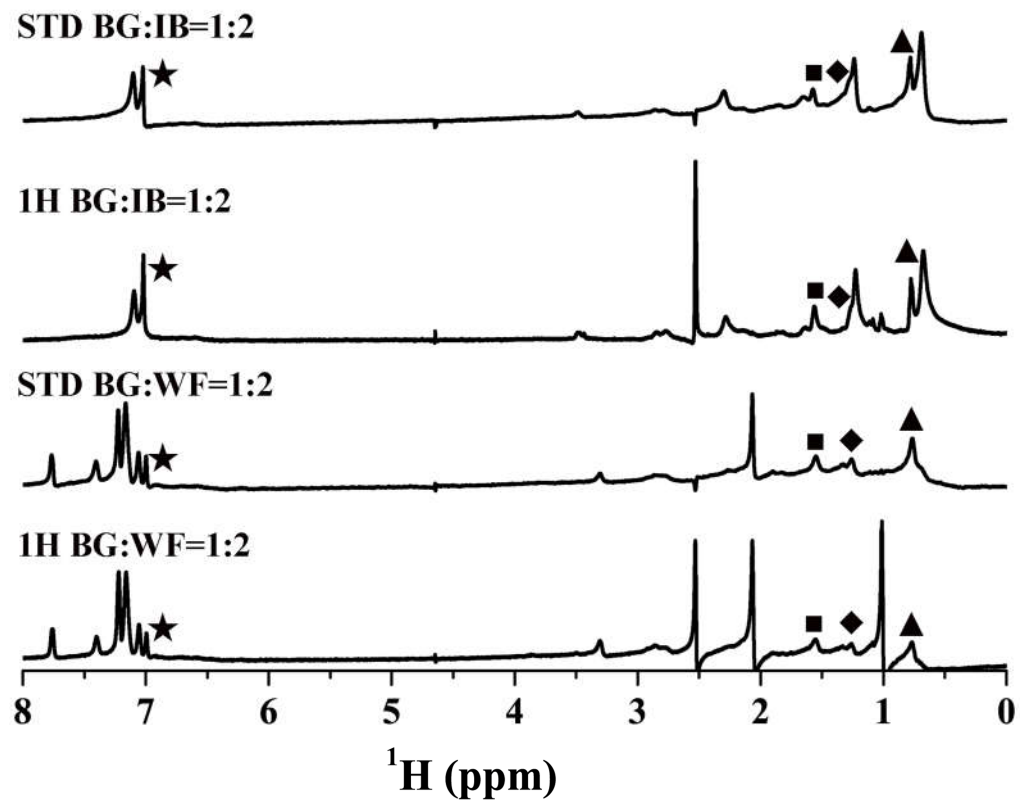


Fig. S9 Effect of WF/IB on the STD spectrum of the BG-HSA interaction. $C_{(\text{HSA})} = 0.01 \text{ mM}$, $C_{(\text{BG})} = 0.4 \text{ mM}$, and $C_{(\text{WF/IB})} = 0.8 \text{ mM}$.

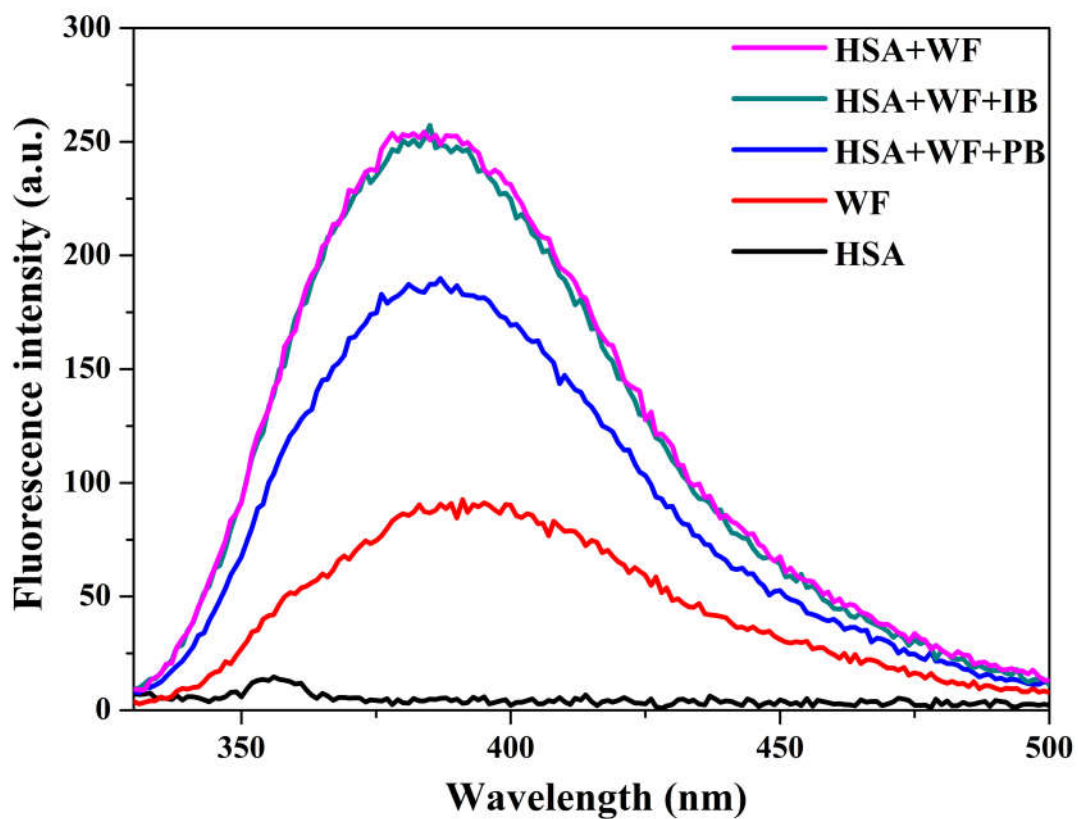


Fig. S10 Effect of PB/IB on the fluorescence of WF–HSA complex ($\lambda_{\text{ex}} = 317 \text{ nm}$).
 $C_{(\text{WF})} = C_{(\text{PB/IB})} = C_{(\text{HSA})} = 2.0 \mu\text{M}$.

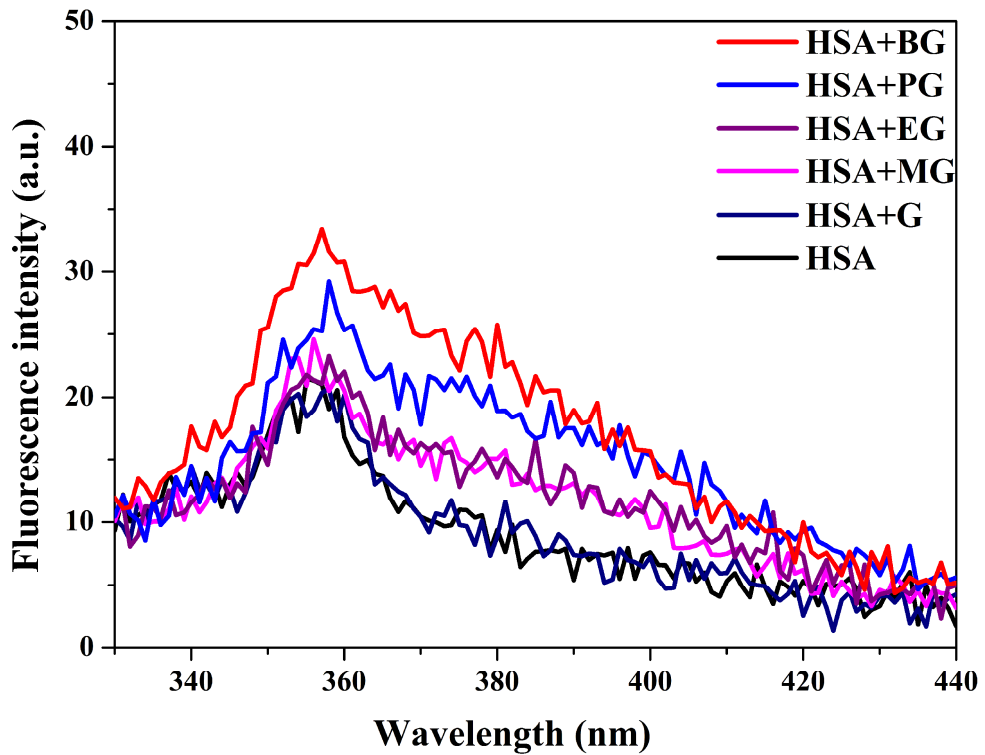


Fig. S11 Fluorescence spectra of G/ME/EG/PG/BG–HSA (A1653) interaction ($\lambda_{\text{ex}} = 317 \text{ nm}$). $C_{(\text{HSA})} = C_{(\text{G/ME/EG/PG/BG})} = 2 \mu\text{M}$.

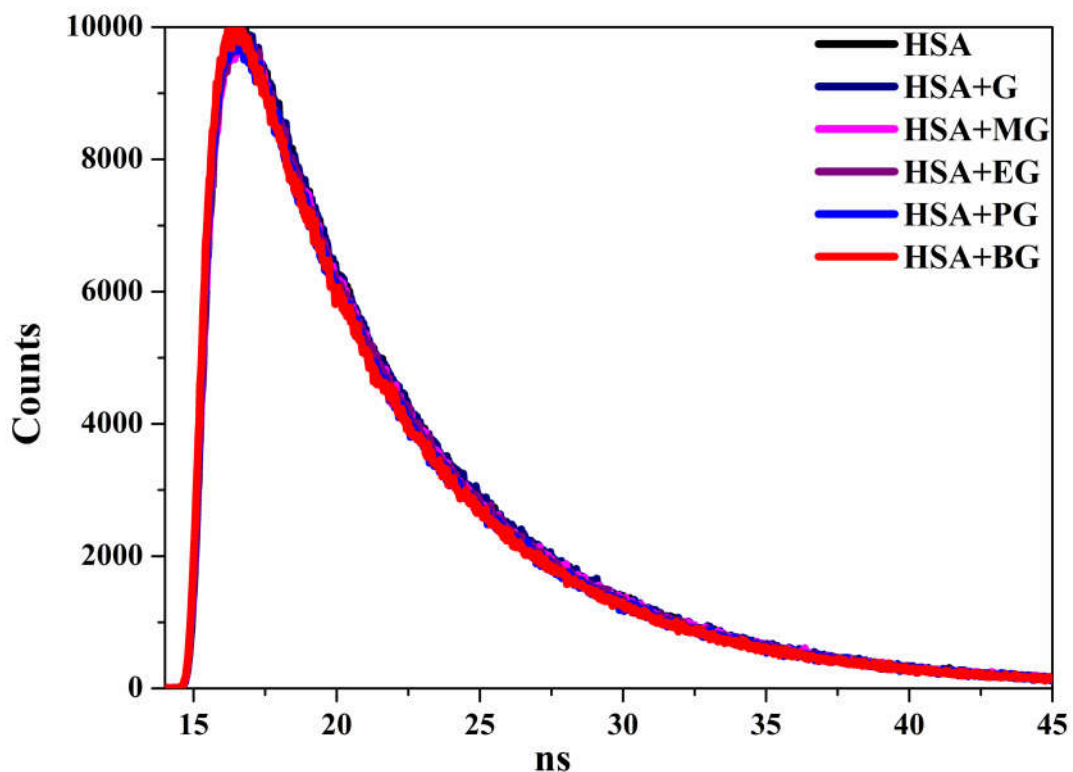


Fig. S12 Fluorescence decay of HSA (A1653) in the absence and presence of probes ($\lambda_{\text{ex}}=280 \text{ nm}$): $C_{(\text{HSA})}=C_{(\text{G/MG/EG/PB/BG})}=2.0 \mu\text{M}$.

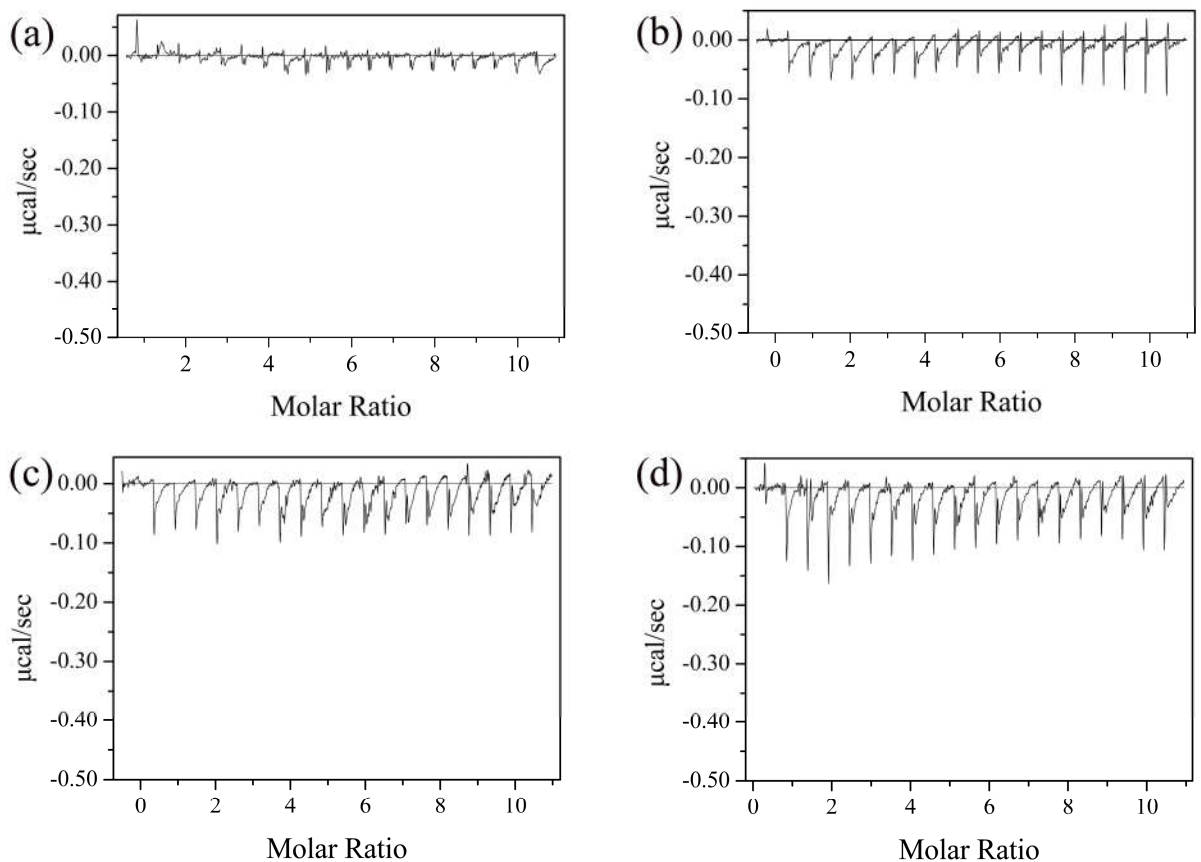


Fig. S13 ITC titration of HSA (A1653)–(a) G/(b) MG/(c) EG/(d) PG interaction.

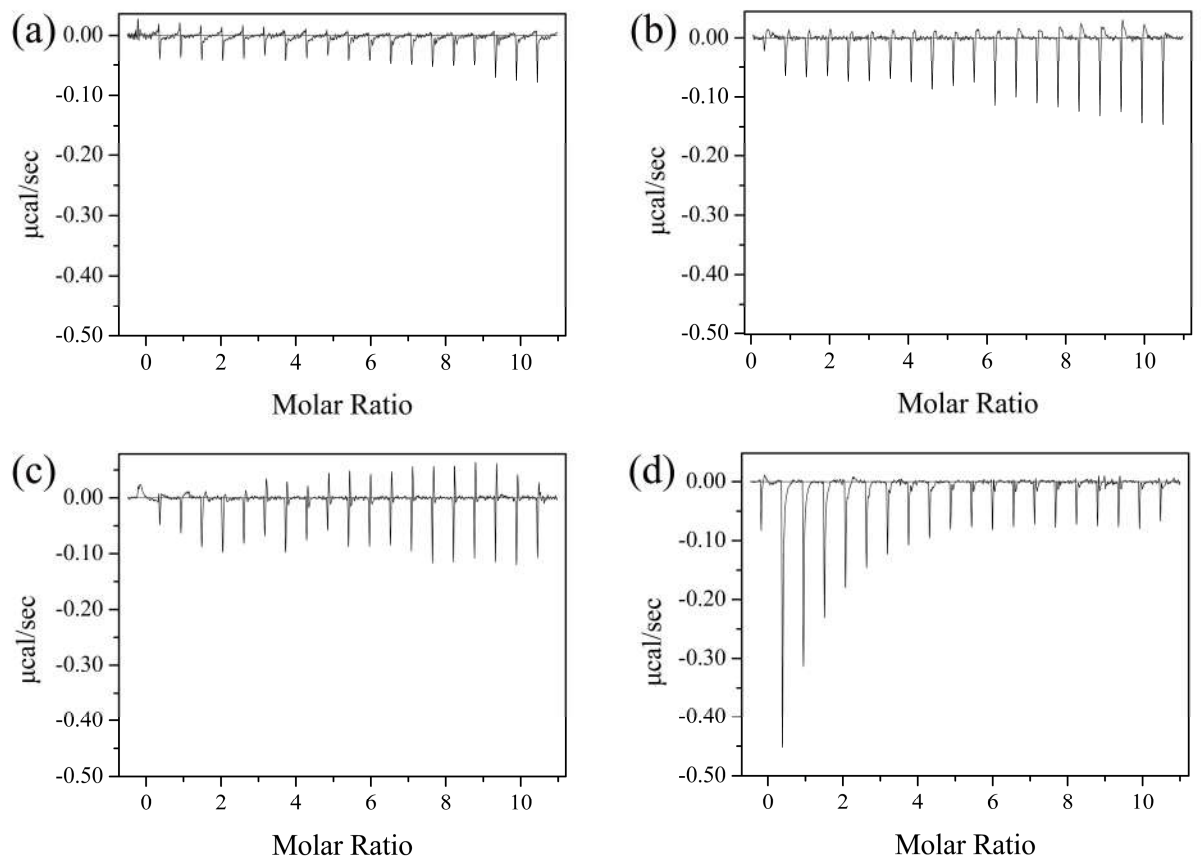


Fig. S14 ITC titration of HSA–(a) G/(b) MG/(c) EG/(d) PG interaction.

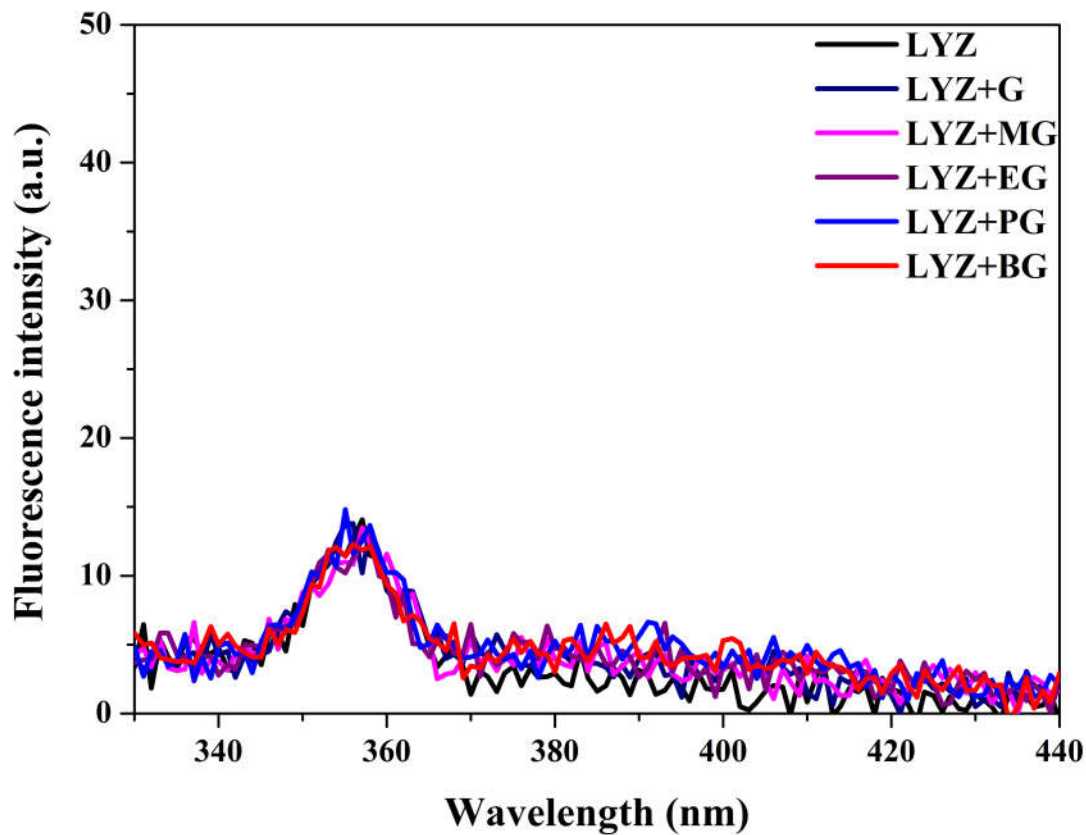


Fig. S15 Fluorescence spectra of G/ME/EG/PG/BG–LYZ interaction ($\lambda_{\text{ex}} = 317 \text{ nm}$).
 $C_{(\text{LYZ})} = C_{(\text{G/ME/EG/PG/BG})} = 2 \mu\text{M}$.

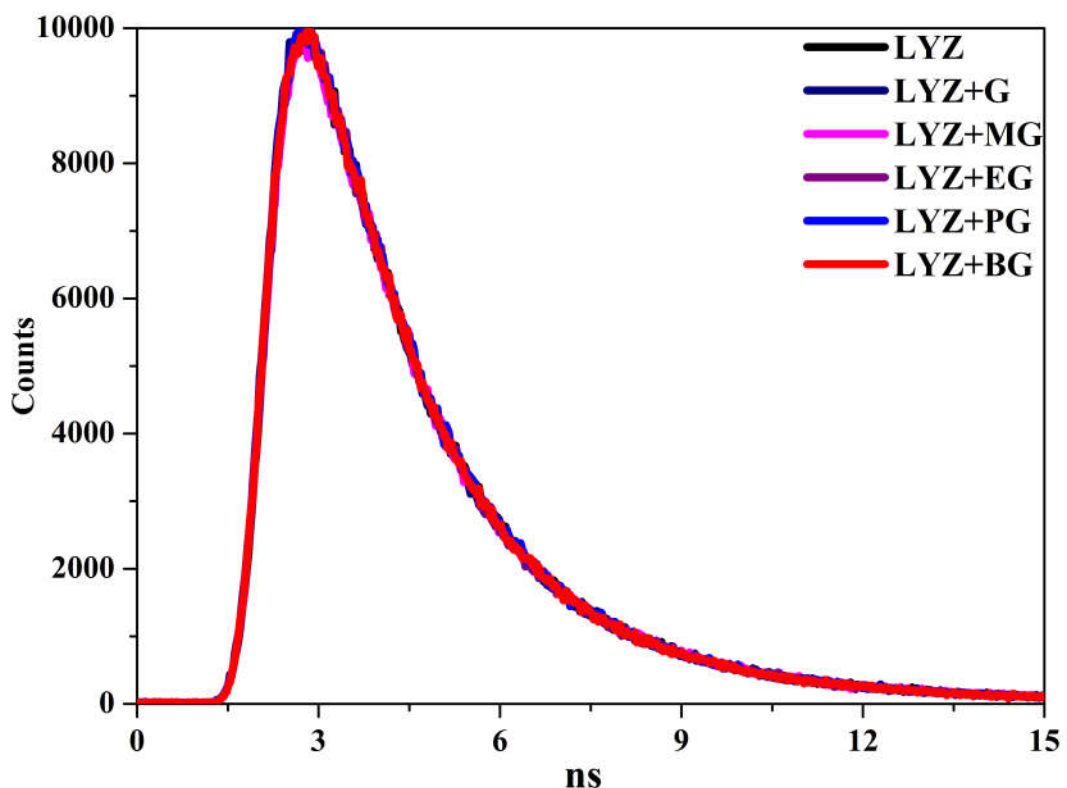


Fig. S16 Fluorescence decay of LYZ in the absence and presence of probes ($\lambda_{\text{ex}}=280$ nm): $C_{(\text{LYZ})}=C_{(\text{G/MG/EG/PB/BG})}=2.0 \mu\text{M}$.

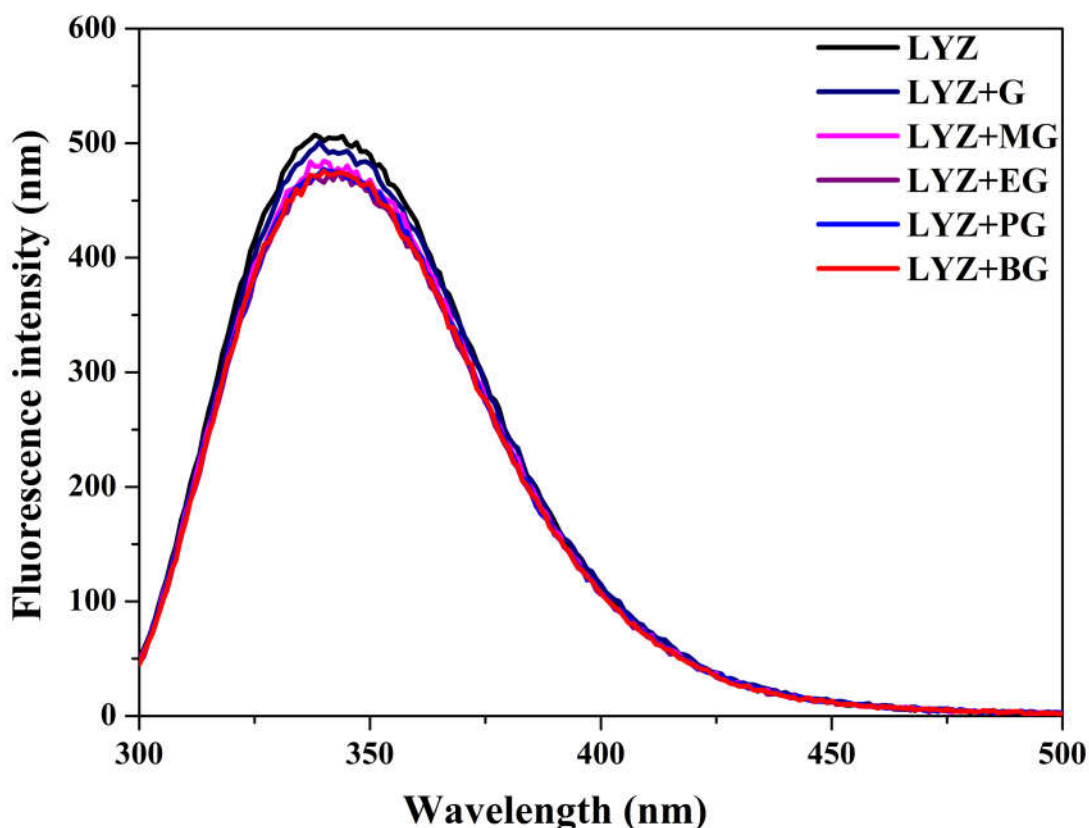


Fig. S17 Fluorescence spectra of G/ME/EG/PG/BG–LYZ interaction ($\lambda_{\text{ex}} = 280 \text{ nm}$).
 $C_{(\text{LYZ})} = C_{(\text{G/ME/EG/PG/BG})} = 2 \mu\text{M}$.

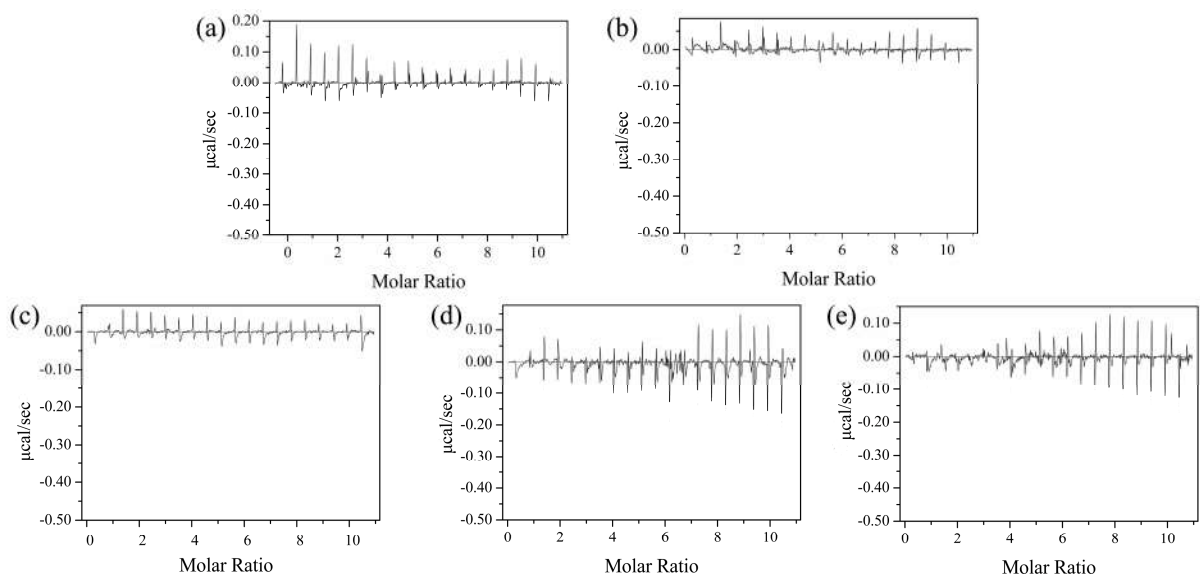


Fig. S18 ITC titration of LYZ–G (a)/MG (b)/EG (c)/PG (d)/BG (e) interaction.

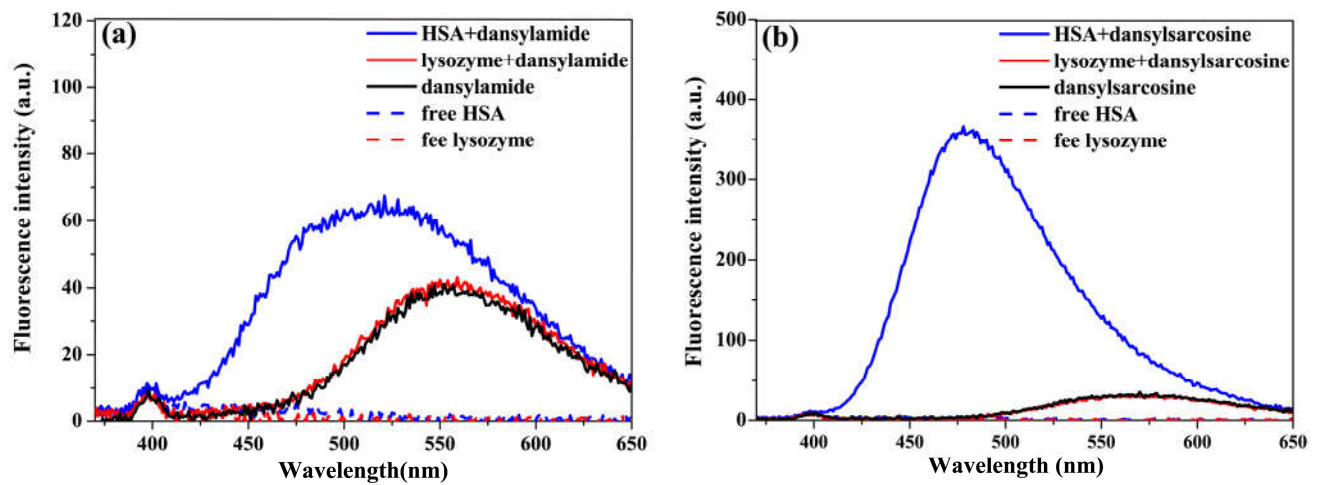


Fig. S19 Fluorescence spectra of dansylamide/dansylsarcosine–HSA/LYZ interaction ($\lambda_{\text{ex}} = 350 \text{ nm}$). $C_{(\text{HSA/LYZ})} = C_{(\text{dansylamide/dansylsarcosine})} = 2 \mu\text{M}$.

Table S1. Lifetime of HSA (A1887) fluorescence decay in the absence and presence of probes.

System	τ_1	τ_2	τ_3	α_1	α_2	α_3	$\langle \tau \rangle$	χ^2
Free HSA	3.399	0.515	6.948	0.334	0.035	0.631	5.539	0.993
G-HSA	3.448	0.485	7.015	0.351	0.040	0.609	5.501	1.028
MG-HSA	3.363	0.436	6.957	0.340	0.032	0.628	5.526	1.072
EG-HSA	3.293	0.464	6.897	0.326	0.050	0.625	5.405	1.107
PG-HSA	2.852	0.456	6.558	0.285	0.184	0.531	4.377	1.045
BG-HSA	2.579	0.449	6.432	0.270	0.282	0.448	3.703	1.131